Available online at www.sciencedirect.com
SCIENCE DIRECT®
ELSEVIER
International Journal of Mechanical Sciences 47 (2005) 1649–1672
International Journal of MECHANICAL SCIENCES
www.elsevier.com/locate/ijmecsci

On the inadequacy of the single-shear plane model of chip formation

Viktor P. Astakhov*

Astakhov Tool Service Co., 3319 Fulham Dr., Rochester Hills, MI 48309, USA

Received 5 July 2004; received in revised form 27 June 2005; accepted 20 July 2005

Abstract

This paper argues that the single-shear plane model is inadequate to the real cutting process. The model has been developed in the late 19th century on the basis of simple observations of the cutting process. Although a number of other models are known to the specialists in this field, the single-shear plane model survived all of them and, moreover, is still the first choice for studies on metal cutting, computer simulations programs and students' textbooks. Although it is usually mentioned that the model represents an idealized cutting process, no information about how far this idealization deviates from reality is provided. This paper lists and discusses the following principal drawbacks of the single-shear plane model: infinite strain rate; unrealistically high shear strain; unrealistic behavior of the work material; improper accounting for the resistance of the work material to cut; unrealistic representation of the tool-workpiece contact; inapplicability for cutting brittle work materials; incorrect velocity diagram; incorrect force diagram; inability to explain chip curling. The paper concludes that any progress in the prediction ability of the metal cutting theory cannot be achieved if the single-shear plane model is still in the very core of this theory.

Keywords: Metal cutting; Theory; Single-shear plane model; Chip formation; Predicted and experimental results

*Corresponding author. Tel.: +1 248 852 0246; fax: +1 419 821 6354.
E-mail address: astvik@lycos.com.
URL: http://www.astvik.com.

0020-7403/$ - see front matter
doi:10.1016/j.ijmecsci.2005.07.002

1. Introduction

Metal cutting, or simply machining, is one of the oldest processes for shaping components in the manufacturing industry. It is estimated that 15% of the value of all mechanical components manufactured worldwide is derived from machining operations. However, despite its obvious economic and technical importance, machining remains one of the least understood manufacturing operations due to low predictive ability of the machining models [1,2].

The old ''trial-and-error'' experimental method, originally developed in the middle of the 19th century (well summarized in [3]) is still in wide use in metal cutting research and development activities. Its modern form, known as the ''unified or generalized mechanics approach'', has been pursued by Armarego and co-workers for years [3] and then spread as the mechanistic approach in metal cutting [4]. It was developed as an alternative to the metal cutting theory because the latter did not prove its ability to solve even simplest practical problems. Some researches even argued about ''advantages of experimental research over theoretical models'' [5].

Although a number of books on metal cutting have been published, none of them provide a critical comparison of different theories of metal cutting in their discussion of the corresponding models of chip formation which constitute the very core of the metal cutting theory. For example, Aramarego and Brown discussed [6] different models of chip formation but did not provide comparison of their adequacy to reality. After reading these books, a practical specialist in metal cutting feels that he is not sufficiently equipped with knowledge on the advantages and drawbacks of different models; so he/she may wonder which particular model of chip formation to use in a given practical case. Besides, a great number of papers were published on the subject providing contradictive results and thus adding even more confusion to the matter.

When one tries to learn the basics of the metal cutting theory, he/she takes a textbook on metal cutting (manufacturing, tool design, etc.) and then reads that the single-shear plane model of chip formation constitutes the very core of this theory. Although a number of other models are known to be specialists in this field, the single-shear plane model survived all of them and, moreover, is still the only option for studies on metal cutting [7], computer simulation programs including the most advanced FEA packages (e.g. [8]) and students' textbooks (e.g. [9,10]). A simple explanation for this fact is that the model is easy to teach, to learn, and simple numerical examples to calculate cutting parameters can be worked out for student's assignments [11]. Although it is usually mentioned that the model represents an idealized cutting process [12] and that quantitatively the shear–angle relationship has been found to be inaccurate (p. 48 in [6]), no information about how far this idealization deviates from reality is provided. It is also interesting that this model was historically the first model developed, then was rejected, and then finally widely accepted remaining 'a paramount' today. Even though a realistic model of chip formation with the curved shear surface, known as the universal slip line model, has been developed and verified by Jawahir, Fang and co-workers [13–17], specialist and practitioners in the field still use the significantly inferior the single-shear plane model.

The objective of this paper is to discuss major drawbacks of the single-shear plane model showing that this model cannot be used in the development of the predictive metal cutting theory as well as in the development of FEA programs and simulations of the metal cutting process.

2. Development of the single-shear plane model

The single-shear plane model and practically all its 'basic mechanics' have been known since the 19th century and, therefore, cannot be, even in principle, referred to as the Merchant (sometimes, the Ernst and Merchant) model. This fact was very well expressed by Finnie [18] who pointed out that while the work of Zvorykin and others, leading to the equations to predict the shear angle in cutting, had relatively little influence on subsequent development, the very similar work of Merchant, Ernst and others almost 50 years later has been the basis of most of the present metal-cutting analyses. Even the well-known visualization of the single-shear plane model, the so-called card model of the cutting process assigned by many books (for example [11]) to Ernst and Merchant, was proposed and discussed by Piispanen years earlier [19,20]. Knowing these facts, one may wonder why Oxley (p. 23 in [21]) stated that "the single-shear plane model is based on the experimental observations made by Ernst (1938)."

The single-shear plane model of chip formation has been constructed using simple observations of the metal cutting process at the end of the 19th century. Time in 1870 [22] presented the results of his observations of the cutting process. The observations seem to have led to an idealized picture, which is known today as the single-shear plane model for orthogonal cutting schematically shown in Fig. 1a. The scheme shows the workpiece moving with the cutting velocity v and a stationary cutting tool having the rake angle γ. The tool removes the stock of

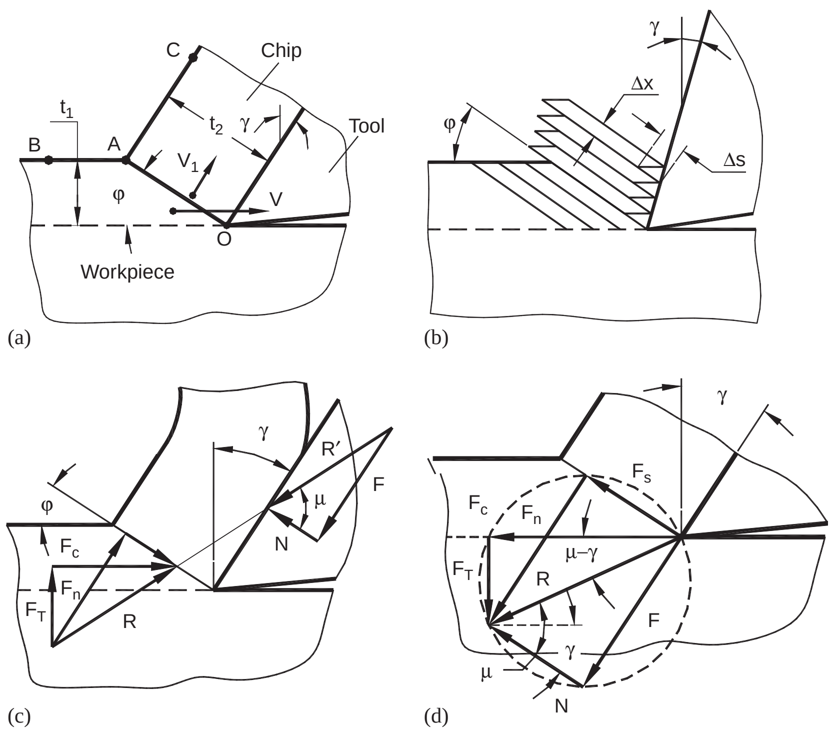

Fig. 1. The single-shear plane model of chip formation: (a) as proposed by Time; (b) Card model approximation due to Piispanen; (c) Merchant's free body diagram for the chip; (d) Merchant's "convenient" free body diagram.

thickness t_1 by shearing it (as was suggested by Time) ahead of the tool in a zone which is rather thin compared to its length and thus it can be represented reasonably well by the shear plane OA. The position of the shear plane is defined by the shear angle φ, as shown in Fig. 1a. After being sheared, the layer being removed becomes the chip having thickness t_2, which slides along the tool rake face. Tresca in 1873 argued [23] that the cutting process is one of compressions of the metal ahead of the tool so the chip failure should occur along the path of tool motion. Time in 1877 provided further evidences that the material being cut is deformed by shearing rather then by compression [24]. As shown by Astakhov [25], there are no contradictions between Time and Tresca approaches. In machining of brittle work materials, the fracture of the layer being removed is due to maximum compressive stress while in the machining ductile materials these compressive stresses cause plastic deformation by shearing resulting in the ductile fracture of this layer. Zvorykin [26] provided physical explanation for this model as follows. The layer being removed of thickness t_1 transforms into the chip of thickness t_2 as a result of shear deformation that takes place along a certain unique plane AO inclined to the cutting direction at an angle φ. The velocity relationship between the cutting velocity, v and the chip velocity, v_1, has been also established in the form used today [12]. Although the discussed work became known in Europe and further European studies on metal cutting referred to these works, they were somehow completely unknown in North America where theoretical studies on the metal cutting theory began years later [27].

As early as 1896, Briks [28] justly criticized the single-shear plane model pointing out that the drawbacks of this model are: the single shear plane and the absence of the smooth connection at point A so that the motion of a particle located in point B into the corresponding location C on the chip is impossible from the point of physics of metal deformation. According to Briks, the existence of a single shear plane is impossible because of two reasons. First, an infinitely high stress gradient must exist in this plane due to instant chip deformation (chip thickness t_2 is usually 2–4 times greater than that of the layer being removed, t_1). Second, a particle of the layer being removed should be subjected to infinite deceleration on passing the shear plane because its velocity changes instantly from v into v_1. Analyzing these drawbacks, Briks assumed that they can be resolved if a certain transition zone, where the deformation and velocity of the work material take place continuously and thus smoothly exists between the layer being removed and the chip. Briks named this zone as the deformation or plastic zone (these two terms were used interchangeably in his work). Unfortunately, these conclusions were much ahead of this time so they were not even noticed by the future researchers until the mid-1950s. Developing the concept of the deformation zone, Briks suggested that it consists of a family of shear planes as shown in Fig. 2. Such a shape can be readily explained if one recalls what type of tool materials was available at the time of his study. Neither high-speed steels nor sintered carbides were yet introduced; thus Briks conducted his experiments using carbon tool steels as the tool material. As a result, the cutting speed was low so that the fanwise shape of the deformation zone shown in Fig. 2 was not that unusual.

To solve the contradictions associated with the single-shear plane model, Briks suggested that the plastic deformation takes place in a certain zone which is defined as consisting of a family of shear planes (OA_1, $OA_2, \ldots, OA_n$) arranged fanwise as shown in Fig. 2. As such, the outer surface of the workpiece and the chip-free surface are connected by a certain transition line A_0A_n consisting of a series of curves A_aA_2, $A_2A_3, \ldots, A_{n-1}A_n$ as a result, the deformation of the layer

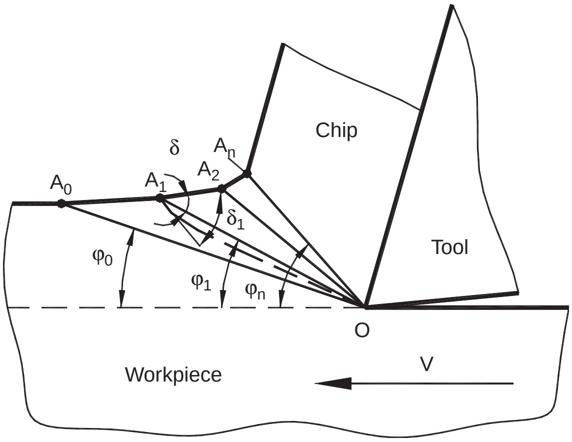

Fig. 2. Briks' model.

being removed takes place step-by-step in the deformation zone and each successive shear plane adds some portion to this deformation. The model proposed by Briks solved the most severe contradictions associated with the single shear plane model. It was also much ahead of the general level achieved at that time.

Zorev [29] analyzing the Briks model, did not mention its advantages. Instead, he pointed out the drawbacks of this model: (a) a microvolume of the workpiece material passing the boundary OA_n must receive infinitely large acceleration, (b) lines $OA_1 - OA_n$ cannot be straight inclined at different angles δ to the transition surface because the boundary condition on the transition surface A_1A_n is so that these lines must form equal angles of $\pi/4$ (angles δ_1 as shown in Fig. 2) with the tangents to this surface in the corresponding points $A_2 - A_n$. Criticizing Briks model, Zorev did not present any metallographic support to his "$\pi/4$" statement even though his book contains a great number of micrographs. Instead, Zorev attempted to construct a slip line field in the deformation zone using the basic properties of slip lines. According to his considerations, the deformation process in metal cutting involves shearing and, therefore, is characterized by the lines of maximum shear stress, i.e. by characteristic curves or slip lines (making this 'logical' statement-assumptions, Zorev automatically accepted that pure shear deformation is the prime deformation mode in chip formation and no strain-hardening of the work material takes place). He considered the deformation zone as superposition of two independent processes, namely, deformation and friction. Utilizing the basic properties of shear lines (term used by Zorev [29]), he attempted to superimpose the slip lines due to plastic deformation and those due to friction at the tool–chip interface.

It should be pointed out here that Zorev's modeling of the deformation zones by slip lines is descriptive and did not follow the common practice of their construction. According to Johnson and Mellor [30], the major feature of the theory of slip lines concerns the manner in which the solution are arrived at. In any case, such a solution cannot be obtained without constructing the velocity hodograph and verifying boundary conditions. Unfortunately, Zorev did not follow this way although it was already applied to the similar problem by Palmer and Oxley [31]. In Zorev's opinion, his qualitative analysis was sufficient to "imagine" an arrangement of the shear lines

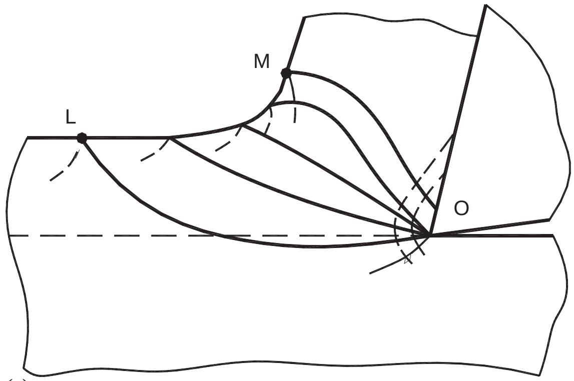

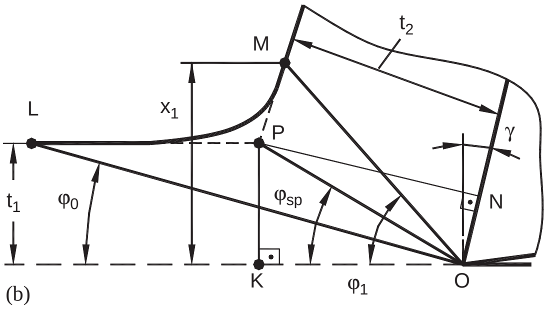

Fig. 3. Zorev's models: (a) a qualitative model; (b) the final simplified.

throughout the whole plastic zone "in approximately the form" shown in Fig. 3a. In the author's opinion, it is next to impossible to figure out the shape of these shear lines knowing only their directions at starting and ending points unless the velocity hodograph is constructed [31,32]. Plastic zone LOM is limited by shear line OL, along which the first plastic deformation in shear occurs; shear line OM along which the last shear deformations occurs; line LM which is the deformed section of the workpiece free surface. The plastic zone LOM includes "a family of shear lines along which growing shear deformations are formed successively" [29]. Zorev stated that such a shape of the deformation (plastic) zone is based on the observations made during multiple experimental studies. Although this model is known in the literature on metal cutting as the Zorev's model, no study points out that no solution for this model was developed so its significance is of qualitative nature.

Trying to build a model around the schematic shown in Fig. 3a, Zorev arrived at a conclusion that there are great difficulties in precisely determining the stressed and deformed state in the deformation zone he constructed using the theory of plasticity. He pointed out that the reasons for this conclusion were as follows: (a) the boundaries of the deformation zone are not set and thus cannot be defined. In other words, there is no steady-state mode of deformation in metal cutting as the shape of the deformation zone is ever changing, and (b) the stress components in the deformation zone do not change in proportion to one another. As a result a several consecutive steps, Zorev was forced to adopt a significantly simplified model shown in Fig. 3b. This model differs from that shown in Fig. 3a in that the curves of the first family of shear lines are replaced by straight lines and, in addition, it is assumed that there no shearing takes place along the second family of shear lines adjacent to the tool rake face. This model is very similar to that proposed by Briks [28] and Okushima and Hitomi [33]. Moreover, this model levels all Zorev's considerations made in the discussion of model shown in Fig. 3a. Trying to deal with this simplified model, Zorev further introduced concepts of 'a specific shear plane' and 'a specific shear angle, φ_{sp}' using purely geometrical considerations. According to Zorev, the specific shear plane is the line 'passing through the cutting edge and the line of intersection of the outer surface of the layer being removed and the chip.' This specific shear plane is represented by line *OP* in Fig. 3b.

Zorev admitted that he finally arrived at the Time model (Fig. 1a) and using a simple geometrical relationship that exists between two right triangles *OKP* and *ONP*, obtained the Time formula for the chip compression ratio ξ

$$\xi = \frac{\cos(\varphi_{sp} - \gamma)}{\sin \varphi_{sp}}. \tag{1}$$

Assuming further that $\varphi_1 \approx \varphi_{sp}$, Zorev obtained expression for the final shear strain as

$$\varepsilon_1 \approx \varepsilon_{sp} \approx \cot \varphi_{sp} + \tan(\varphi_{sp} - \gamma) \tag{2}$$

or expressed through the chip compression ratio $\zeta = t_2/t_1$ and tool rake angle γ, it becomes

$$\varepsilon_1 \approx \varepsilon_{sp} = \frac{1 - 2\zeta \sin \gamma + \zeta^2}{\zeta \cos \gamma}. \tag{3}$$

Zorev mentioned that because $\varphi_{sp} < \varphi_1$ and $t_1 < x_1$, (p. 49 in [29]) Eq. (3) gives somewhat 'enhanced' values for deformation.

Zorev admitted that relationships (1)–(3) were well known in reference sources as derived directly from an examination of the single shear plane model. However, the way they were derived in Zorev's book gives a more general solution from which other known models can be obtained. Using pure geometrical considerations, Zorev was able to obtain a generalized solution of the following form

$$2\varphi_{sp} + \theta - \gamma \approx \frac{\pi}{2} - \psi_{sp}. \tag{4}$$

Zorev showed that all the known solutions for the specific shear angle could be obtained from this equation. For the single-shear plane model, the tangent drawn to the workpiece free surface at point *P* (Fig. 3b) is a horizontal line and thus $\psi_{sp} = 0$. Substitution of this value into Eq. (4) yields

$$2\varphi_{sp} + \theta - \gamma = \frac{\pi}{2}, \tag{5}$$

which is the known Ernst and Merchant solution [34]. Using the notations $\psi_{sp} = c_1$ and $(\pi/2 - \gamma) = \delta$, the known Zvorykin solution [26] is obtained

$$\varphi_{sp} = \frac{\pi}{2} - \frac{\theta + c_1 + \delta}{2}. \tag{6}$$

Using the notations $\psi_{sp} = c_1$ and $(\pi/2) - c_1 = c$, the modified Merchant solution [35] is obtained

$$2\varphi_{sp} + \theta - \gamma = c. \tag{7}$$

If $\psi_{sp} = \theta - \gamma$, then the Lee and Shafer solution [36] is obtained

$$\varphi = \frac{\pi}{4} + \gamma - \theta \tag{8}$$

and so on.

Analyzing these results, Zorev came to the conclusion that all solutions related to Eq. (4) are formal and based on pure geometrical considerations known since the 19th century and thus they have little to do with the physics or even mechanics of metal cutting because no physical laws (besides the law of simple friction at the tool–chip interface) and/or principles of mechanics of materials have been utilized in the course of the development of the discussed models.

3. Merchant's modifications

3.1. Card model

According to Merchant, the so-called card model of the cutting process proposed by Piispanen [19] is very useful to illustrate the physical significance of shear strain and to develop the velocity diagram of the cutting process. This model is shown in Fig. 1b. The card-like elements displaced by the cutting tool were assumed to have a finite thickness Δx. Then each element of thickness Δx is displaced through a distance Δs with respect to its neighbor during the formation of the chip. Therefore, shear strain ε can be calculated as

$$\varepsilon = \frac{\Delta s}{\Delta x} \tag{9}$$

and from geometry of Fig. 1b it can be found that

$$\varepsilon = \cot \varphi + \tan(\varphi - \gamma). \tag{10}$$

Although the card model is used almost in each textbook on metal cutting to explain chip formation, this model has never been considered with the time axis. Such a consideration is shown in Fig. 4 where the sequence of the formation of two card-like chip elements is illustrated. Let AB be the shear plane and point A is the initial point of consideration in frame 1. Due to the penetration force P, the first chip fragment $ABCD$ is formed although it does not separate from the workpiece along AD yet (frame 2). Further tool penetration results in the separation of AD from the workpiece. As such, point A on the chip separated from point A' on the workpiece and point D from D' (frame 3). Then chip fragment $ABCD$ slides along the shear plane (violating practically all the postulates of the mechanics of continuous media) until the cutting edge reaches point D' (frame 4). A new chip fragment $D'GFE$ starts to form (frame 5). Then, point D' on the chip separates from point D'' on the workpiece and point E on the chip separates from point E' (frame 6). Then the process repeats itself.

It should be evident that the separation of the chip fragment from the workpiece is possible if and only if the stress along plane represented in 2D by lines AD, $D'E$, etc. exceeds the strength of the work material and the strain along this plane must exceed the strain at fracture. In other words, the crack, as the result of separation chip fragments along the direction of tool motion, should form in front of the cutting edge as suggested by Reuleaux in 1900 [37] whose work was

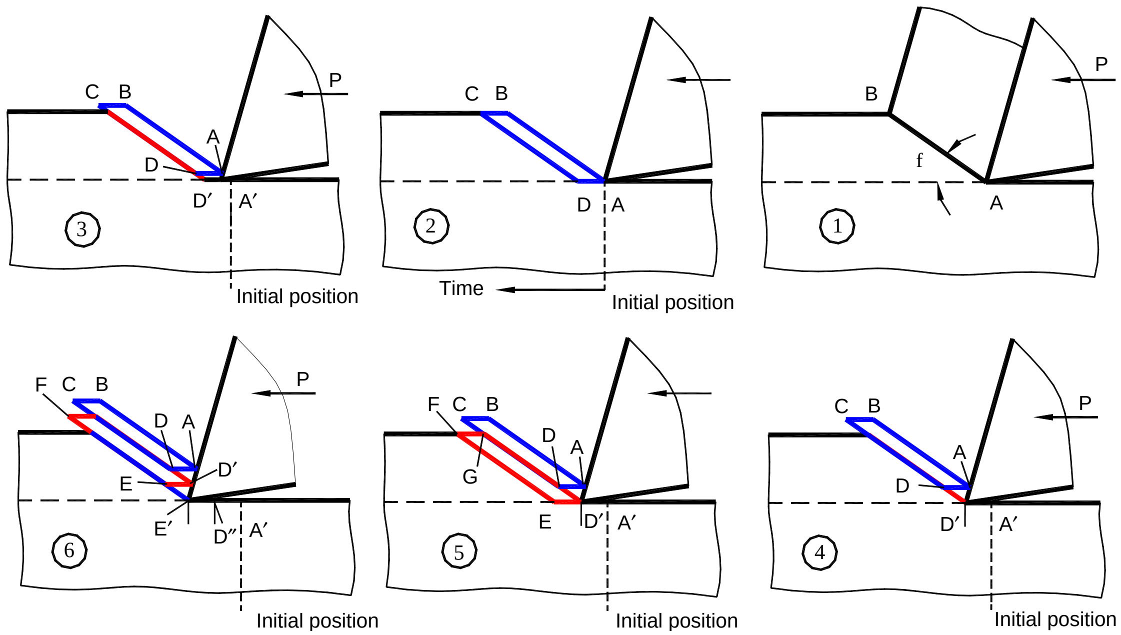

Fig. 4. Card model with the time axis.

cruised vigorously by subsequent researchers. Although Merchant pointed out [35] that thickness $\Delta x \to 0$ in real cutting process, the fracture would take place even for infinitesimal thickness of a chip fragment. Recently, Atkins in his very extensive analysis of the problem [38] pointed out that the fracture must occur along the surface separating the layer being removed and the rest of the workpiece. However, what is not pointed out is that if the state of stress ahead of the tool is determined using the discussed model then the discussed fracture can never occur in this direction.

3.2. Velocity diagram

When the single-shear plane model was first introduced and discussed, only the tool v and chip $v_1 = v_F$ (v_F designation is kept in this section instead of v_1 as was introduced by Merchant [35]) velocities were considered as shown in Fig. 1a. Using the above-discussed card model, Merchant developed the velocity diagram shown in Fig. 5a (similar to that suggested earlier by Zvorykin [26]), which is in almost exclusive use in the modern literature related to metal cutting. Merchant [35] defined v_S is the velocity of shear (p. 270 in [35]) and then used this velocity to calculate the work done in shear per unit volume as $W_S = F_S v_S / A_c v_S$ where F_S is the force acting along the shear plane and $A_c (= t_1 d_w)$ is the uncut chip cross-sectional area. Shaw transformed this formula to calculate the shear energy (Eq. (3.26) in [12]). Shaw [12] and Oxley [21] suggested to calculate the rate of strain in metal cutting as

$$\dot{\gamma} = \frac{v_S}{\Delta y}, \tag{11}$$

where Δy is the conditional thickness of the shear zone (or plane as per Shaw [12]).

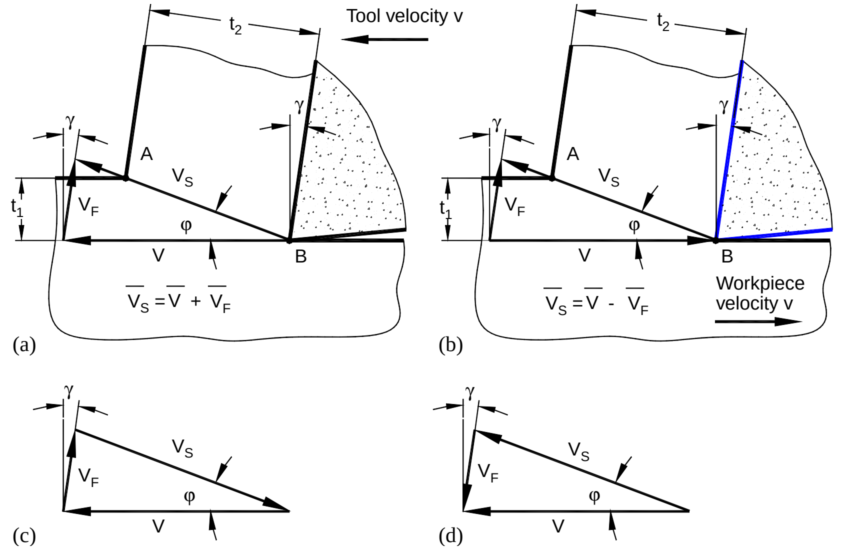

Fig. 5. Velocity diagrams: (a) Merchant's diagram: the tool moves with the cutting velocity v and the workpiece is stationary; (b) the tool is stationary and the workpiece moves with the cutting velocity v; (c) velocity diagram used by Black; (d) velocity diagram by Stephenson and Agapiou.

Using the developed velocity diagram (Fig. 5a), Merchant concluded [35] that

$$\vec{v}_S = \vec{v} + \vec{v}_1. \tag{12}$$

However, if one considers the kinematically equivalent model where the workpiece moves with the cutting velocity while the tool is stationary [11,39] as shown in Fig. 5b, then Eq. (12) is no more valid. Rather it becomes

$$\vec{v}_S = \vec{v} - \vec{v}_1. \tag{13}$$

If it is so then all the basic widely used metal cutting relationships obtained using Eq. (12) are not valid for the considered case. Obviously, the models shown in Figs. 5a and b are kinematically equivalent so the magnitude and direction of the shearing velocity MUST be the same. This, however, does not follow from the comparison of the discussed velocity diagrams.

The problem with the velocity diagram was noticed by some researches who tried to introduce some corrections to this diagram in order to match the known vectorial summation as pointed out by Astakhov [40]. For example, Black [41,42] "silently" corrected the velocity diagram shown in Figs. 5a and b offering his version shown in Fig. 5c. The same diagram was used by Altintas in his book [43]. Although this corrected velocity diagram solves the "sign" problem and this made the derivation of basic kinematic equations correct, the cutting process according to this velocity diagram becomes an energy generating, rather than an energy consuming, process. This is because the shear velocity, v_S, and shear force, F_S, have opposite directions. Trying to resolve the discussed "sign" problem, Stephenson and Agapiou [44] proposed the velocity diagram shown in Fig. 5d, where the direction of chip velocity is assumed to be opposite to the direction of its motion. Obviously, this is in direct contradiction with simple observations of the chip formation process where the chip moves from the chip formation zone.

It directly follows from Fig. 5a that the shear velocity is calculated as $v_S = (\cos\gamma/\cos(\varphi-\gamma))v$ and the velocity normal to the shear plane is calculated as $v_n = v\sin\varphi$ so the shear strain that represents chip plastic deformation is calculated as

$$\varepsilon = \frac{v_S}{v_n} = \frac{\cos\gamma}{\cos(\varphi-\gamma)\sin\varphi} = \frac{1-2\zeta\sin\gamma+\zeta^2}{\zeta\cos\gamma}. \qquad (14)$$

Although Eqs. (11) and (14) are used in practically all books on metal cutting, there are some obvious problems with these equations in terms of physical meaning and experimental confirmation:

- Because v_S is great and, according to Fig. 5a, may well exceed the cutting velocity when the tool rake angle γ is negative (for example, Fig. 9 in [45]), the calculated strain rate in metal cutting was found to be in a range of 10^4–$10^6\,\mathrm{s}^{-1}$ or even higher. It is important to realize that this conclusion was made when the experimental technique for measuring material properties and behavior at high strain rates was not yet well developed [25]. Today such a technique is common in material testing and thus the data on the behavior of various materials at high strain rates are widely available [46,47], it can be stated that multiple experimental evidences and test results conducted at low, normal [29] and even ultra-high cutting speeds [48] do not support (both mechanically and metallurgically) the claim about this high strain rate in metal cutting.
- If one calculates shear strain using Eq. (14) (it can be easily accomplished by measuring the actual chip compression ratio, ζ) and then compares the result with the shear strain at fracture obtained in standard materials tests (tensile or compression), he easily finds that the calculated shear strain is much greater (2–5 folds) than that obtained in the standard materials tests. Moreover, when the chip compression ratio $\zeta = 1$, i.e. the uncut chip thickness is equal to the chip thickness so that no the plastic deformation occurs in metal cutting [49], the shear strain, calculated by Eq. (14), remains very significant. For example, when $\zeta = 1$, the rake angle $\gamma = -10^\circ$, Eq. (14) yields $\varepsilon = 2.38$; when $\zeta = 1$, $\gamma = 0^\circ$ then $\varepsilon = 2$; when $\zeta = 1$, $\gamma = +10^\circ$ then $\varepsilon = 1.68$. This severe physical contradiction cannot be resolved with the existent velocity diagram.
- Multiple known results of the experimental studies of the deformation of the layer being removed using microcoordinate grid scribed of the side of the workpiece do not support the discussed velocity diagram and the existence of unique shear plane. These results are well analyzed by Zorev (p. 7 in [29]). Black and Huang [41] and Payton and Black [50] presented the results of SEM studies showing that the actual shear velocity as a component of the chip velocity in the deformation zone is rather small (Figs. 10 and 11 in [41] and 5 in [50]).

To understand why the velocity diagram shown in Fig. 5a is incorrect, one should properly define the meaning of the term "velocity." It is clear that the velocity is a vector so it has magnitude and direction. These two characteristics are not violated in the known velocity diagrams. What was completely ignored in these diagrams is the fact that the velocity as a vector makes sense if and only if it is defined with respect to a reference point or coordinate system. Unfortunately, not a single literature source defines such a point or a system.

Consider the single-shear plane model as shown in Fig. 6a. The stationary xy-coordinate system is set as shown in this figure. In this coordinate system, the tool moves with velocity $\vec{v}$ from left to right along the x-axis and the workpiece is stationary with respect to the introduced coordinate system. According to Merchant [35], the chip, the workpiece and the tool are rigid bodies having only translation velocities. Therefore, as it is known from kinematics, all points of the chip MUST have the same velocity. Consider a point $\boldsymbol{M}_{ch}$ located on the chip contact side. Point $\boldsymbol{M}_{ch}$ on the chip and point $\boldsymbol{M}_t$ on the tool are coincident points at the moment of consideration. The condition of their contact in terms of velocities is: $\vec{v}_{x-M_{ch}} = \vec{v}_{x-M_t}$. Besides, the velocity of point $\boldsymbol{M}_{ch}$ with respect to the cutting tool is known to be v_F as shown in Fig. 6a (wrongly termed as the chip velocity in practically all known literature sources). Therefore, the real chip velocity in the stationary xy-coordinate system can be determined as the vectorial sum of the mentioned velocity components as $\vec{v}_{ch} = \vec{v}_F + \vec{v}$. As seen in Fig. 6a, as the tool moves, point $\boldsymbol{M}_{ch}$ moves in the direction of the chip velocity v_{ch} consequently occupying positions $\boldsymbol{M}'_{ch}$, $\boldsymbol{M}''_{ch}$, $\boldsymbol{M}'''_{ch}$, $\boldsymbol{M}''''_{ch}$, etc.

Consider two pairs of coincident point located at the ends of the shear plane: points A_w (belongs to the workpiece) and A_{ch} (belongs to the chip); points B_w (belongs to the workpiece) and B_{ch} (belongs to the chip) shown in Fig. 6b. Because these points remain coincident as the tool moves as shown in Fig. 6a by points A, A', A'', A''', A'''' and B, B', B'', B''', B'''', respectively, they must have the same velocity along the x-axis as required by the continuity conditions [25]. In other words, the low shore of the shear plane also moves with velocity v. This is also obvious from Fig. 6a that the shear plane moves with the cutting velocity from left to right as the tool moves.

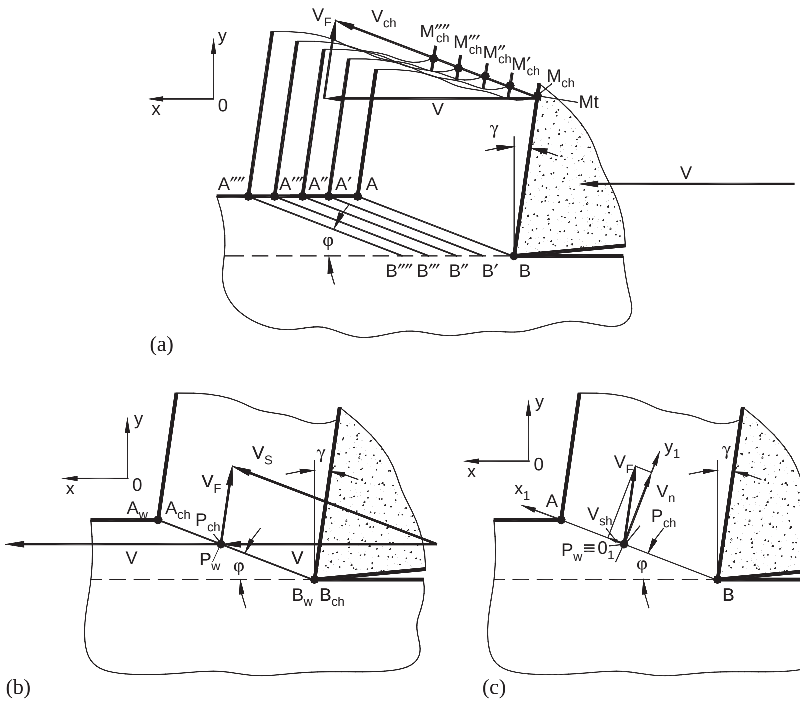

Fig. 6. Analysis of the velocity diagram: (a) Successive displacements of point M_{ch} and its velocity components; (b) velocities of coincident points P_{ch} and P_w; (c) the true shear velocity.

Consider two coincident points: point P_w, which locates on the lower shore of the shear plane and thus belongs to the workpiece, and point P_{ch}, which locates on the upper shore of the shear plane and thus belongs to the chip as shown in Fig. 6b. Point P_{ch} belongs to the chip and thus its velocity is defined the same as that of point $\boldsymbol{M}_{ch}$. Because the lower shore AB of the shear plane moves as a rigid body, point P_w has velocity $\vec{v}$ as shown in Fig. 6a. To find the true shear velocity, one should fix one of the two shores of the shear plane. To do this, the moving x_1y_1-coordinate system is set as shown in Fig. 6c. The x_1-axis of this system is along the shear plane while its y_1-axis is perpendicular to the shear plane. The origin 0_1 coincides with point P_w so it moves with velocity $\vec{v}$ with respect to the xy-coordinate system. It obvious that the chip is the only moving component in this new coordinate system so its velocity $\vec{v}_F$ is to be considered. The projections of vector $\vec{v}_F$ into coordinate axes of the x_1y_1-system are shown in Fig. 6c. As seen they are the normal velocity of the chip, v_N and the velocity v_{sh} with which the chip moves along the shear plane, i.e. the true shear velocity if one assumes that the single-shear model is valid. This conclusion can be supported by experimental observations made by Black and Huang [41] and Payton and Black [50].

3.3. Force diagram

Merchant, considering forces acting in metal cutting, arrived at the force system shown in Fig. 1c (Fig. 7 in [35]). In this figure, the total force is represented by two equal, opposite forces (action and reaction) R and R' which hold the chip in equilibrium. The force, R', which the tool exerts on the chip is resolved into the tool face-chip friction force F and normal force N. The angle μ between F and N is thus the friction angle. The force, R, which the workpiece exerts on the chip is resolved along the shear plane into the shearing force, F_S which, in Merchant's opinion, is responsible for the work expended in shearing the metal, and into normal force F_n, which exerts a compressive stress on the shear plane. Force R is also resolved along the direction of tool motion into F_c, termed by Merchant as the cutting force, and into F_T, the thrust force. Although this diagram looks logical, there are a number of concerns about its physical justification:

3.3.1. Direction of the total cutting force R

First, the friction angle, μ used in its construction and assumed to be constant over the tool–chip interface is way too great. In most engineering and physical situations, friction effects are described by a constant coefficient of Coulomb friction f as

$$f = \tan\mu = F/N. \tag{15}$$

Although it is well-established that contact between two bodies is limited to only a few microscopic high points (asperities), it is customary to calculate stresses by assuming that the forces are distributed over the total (apparent) area A_{ct}. Such an approximation, however, is not far from reality at the tool–chip interface where the actual and apparent contact areas are almost the same due to high contact pressures. Thus the stress normal to interface is $\sigma_c = N/A_{ct}$ called the normal contact stress and the shear (frictional) stress at the interface is $\tau_c = F/A_{ct}$ so that Eq. (15) becomes

$$f = \tau_c/\sigma_c. \tag{16}$$

Eq. (16) reveals that if the friction coefficient at the tool–work interface is constant, the ratio of the shear and normal contact stresses should be the same along the entire tool-chip contact length l_c.

As discussed by Dieter [51], the above analysis was for sliding friction at the interface, as in our first encounter with friction in elementary physics. At the other extreme, one can envision a situation where the interface has a constant film shear strength τ_i. The most usual case is sticking friction, where there is no relative motion between the chip and the tool at their interface. For sticking friction $\tau_I = k$, the flow stress in shear. With von Mises' yield criterion, the coefficient of friction under sticking conditions is

$$f = \frac{k}{\sigma_o} = \frac{\sigma_o/\sqrt{3}}{\sigma_o} = 0.577. \tag{17}$$

Therefore, the value of the friction coefficient f defined by Eq. (17) should be considered as the limiting value so that if $f \geqslant 0.577$ no relative motion can occur at the interface. When $f = 0.577$, the friction angle $\mu = \arctan 0.577 \approx 30^\circ$. Because the chip moves over the tool–chip interface, this angle is even smaller. As such, the normal force, $N = \int_0^{l_c} \sigma_c \, \mathrm{d}A_{ct}$ is much greater than the friction $F = \int_0^{l_c} \tau_c \, \mathrm{d}A_{ct}$ because the normal stress is much greater than the shear stress over the tool–chip interface as supported by multiple theoretical results and experimental evidences [29,52–55]. If it so, the line of action $R - R'$ may not even intersect the actual shear plane.

As follows from the foregoing analysis, if $f \geqslant 0.577$ then no relative motion can occur at the tool–chip interface. In the practice of metal cutting, however, this is not the case. In experimental studies, Zorev [29] obtained $\mu_f = 0.6 - 1.8$, Kronenberg [56]-$0.77 - 1.46$, Armarego and Brown [6]-$0.8 - 2.0$, Finnie and Shaw [57]-$0.88 - 1.85$, Usui and Takeyama [58]-$0.4 - 2.0$, etc. In the simulations of metal cutting, Stenkowsky and Moon [59] used $\mu_f = 0.2$, Komvopoulos and Erpenbeck [60]-$0.0 - 0.5$, Lin et al. [61]-0.074, Lin and Lin [62]-0.001, Stenkowsky and Carroll [63]-0.3, Endres et al. [64]-0.05, 0.10, 0.25, and 0.5, Olovsson et al. [65]-0.1, etc. As seen, the reported values of f obtained in metal cutting tests are well above 0.577. On the other hand, the values of f used in modeling (more often, in FEM modeling), are always below the limiting value to suit the sliding condition at the interface. Interestingly, the results of FEM modeling were always found to be in good agreement with the experimental results regardless of the particular value of the friction coefficient selected for such a modeling.

3.3.2. Stress distribution over the tool–chip interface

If the friction coefficient is constant over the tool–chip interface as assumed by Merchant and subsequent researches then, according to Eq. (16), the distributions of the normal and shear stresses should be equidistant over this interface, i.e. the shapes of the normal and shear stress distributions over the tool–chip interface should be the same. This fact, however, has never been mentioned in the literature on metal cutting so practically all models of the metal cutting process, including the known FEA, were carried out with a constant friction coefficient. The available theoretical and experimental data [29,53,66,67] do not support this assumption.

A far more important issue is that Merchant shifted the resultant cutting force R' parallel to itself (compare Figs. 1c and d) applying it to the cutting edge "for convenience" (p. 272 in [35]). As such the moment equal to this force times the shift distance was overlooked. Unfortunately, this simple flaw was not noticed by the many subsequent researchers who just copied these two pictures. Moreover, the force diagram shown in Fig. 1d became known as the classical Merchant force circle and is discussed today in any book on metal cutting. No wonder that all attempts to apply the fundamental principles of engineering plasticity [68], the principle of minimum energy [35,69], or define the uniqueness of the chip formation process [70] did not yield in any meaningful results because the incomplete force system, shown in Fig. 1d was used as the model.

Using Oxley's ideas about force arrangement in metal cutting and a possibility of the existence of the additional moment, Astakhov proved theoretically and experimentally that this missed moment is the prime cause for chip formation and thus distinguishes the cutting process among other deforming processes [25].

According to the force diagram shown in Fig. 1d, the chip should never separate from the tool rake face because there in no one force factor is responsible for chip curling. Moreover, if the concept of the secondary deformation zone adjacent to the tool rake face is used in the considerations of the single-shear plane model as in practically all known publications on metal cutting (for example [6,12,21,29]) starting from Ernst [71], then the chip contact layer is subjected to further plastic deformation up to seizure as suggested by Trent [72]. As such, the formed chip should curve "inside" the tool rake face because the chip layers adjacent to the chip free surface move freely, i.e. without any further plastic deformation. Unfortunately, these deductions from the single-shear plane model fail to even remotely resemble reality. The chip has rather limited contact area with the tool rake face so that chip curling always occurs even in the simplest case of orthogonal cutting as was presented by Ernst [71] (Fig. 7a). Moreover, it is observed every day by anyone watching any kind of machining.

In the author's opinion, the prime reason for chip curling directly follows from the discussed missed bending moment in the construction of the force diagram shown in Fig. 1d. A model, shown in Fig. 7b is to clarify the issue. The resultant force R is resolved into two components: normal N and compressive F forces. As seen, $N = R\cos\beta$ and $F = R\sin\beta$. The compressive force, F forms the uniform (at least, theoretically) compressive stresses σ_c at the root of the partially formed chip-cantilever known as the primary deformation zone, while the normal force

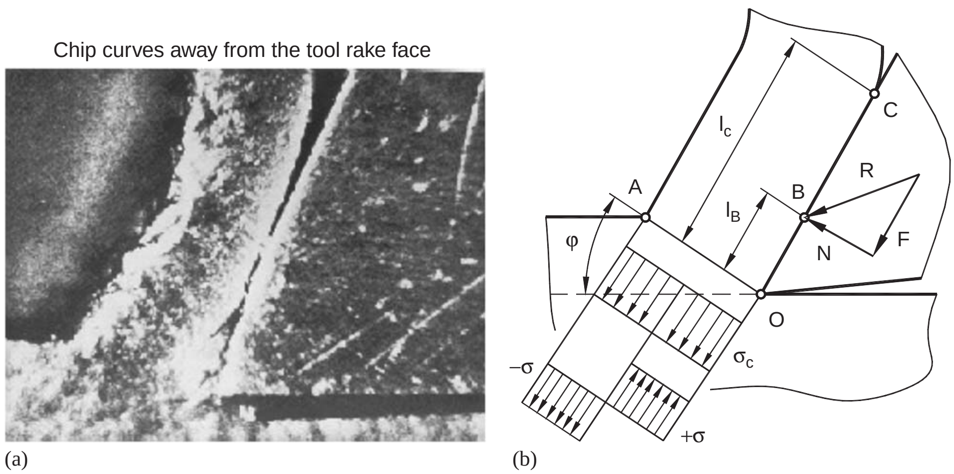

Fig. 7. Chip curling: (a) Ernst observation; (b) model showing the action of the bending moment.

imposes the bending moment $M = NL_c$. This moment causes the compressive stresses ($-\sigma$) at the region of the chip-free surface and the tensile stresses ($+\sigma$) at the chip side that separates from the rest of the workpiece. This state of stress causes chip curling as the chip is "born" with the instilled non-uniform stress distribution. The similar result was obtained by Jawahir et al. [13–17] although from a different viewpoint. The similarity, however, is in the recognition of non-uniform chip deformation on its formation as apposed to the uniform shear stress and strain along the straight shear plane according to the single-shear plane model.

3.4. Resistance of the work material and power spent in cutting

The foundation of the force and energy calculations in metal cutting is based upon determination of the shearing force, F_s using the equation proposed by Ernst and Merchant in 1941 [34]

$$F_s = \frac{\tau_y A_c}{\sin\varphi}, \tag{18}$$

where $A_c = t_1 b_c$ is the uncut chip cross-sectional area (b_c is the width of cut) and τ_y is the shear strength of the work material. According to Ernst and Merchant, the work material deforms when the stress on the shear plane reaches the shear strength of the work material. Later researches published a great number of papers showing that τ_y should be thought of as the shear flow stress which is somehow higher than the yield strength of the work material depending on particular cutting conditions (an extensive analysis of the various approaches to determine the shear flow stress was presented by Astakhov [73]). Still, this stress remains today the only relevant characteristic of the work material characterizing its resistance to cutting [25].

It follows from Fig. 1d that

$$F_c = \frac{F_s\cos(\theta-\gamma)}{\cos(\varphi+\theta-\gamma)} \tag{19}$$

and combining Eqs. (18) and (19), one can obtain

$$F_c = \frac{\tau_y A_c\cos(\theta-\gamma)}{\sin\varphi\cos(\varphi+\theta-\gamma)}. \tag{20}$$

The work spent in cutting is calculated as

$$U_c = F_c v, \tag{21}$$

where v is the cutting velocity. This work spent in cutting defines the energy required for cutting, cutting temperatures, plastic deformation of the work material, machining residual stress and other parameters.

However, everyday practice of machining shows that these considerations do not match reality. For example, machining of medium carbon steel AISI 1045 (tensile strength, ultimate $\sigma_R = 655\,\text{MPa}$, tensile strength, yield $\sigma_{y0.2} = 375\,\text{MPa}$) results in much lower total cutting force (Fig. 8), greater tool life, lower required energy, cutting temperature, machining residual stresses than those obtained in the machining of stainless steel AISI 316L ($\sigma_R = 517\,\text{MPa}$; $\sigma_{y0.2} = 218\,\text{MPa}$) [74]. The prime reason is that any strength characteristic of the work material in terms of its characteristic stresses cannot be considered alone without corresponding strains,

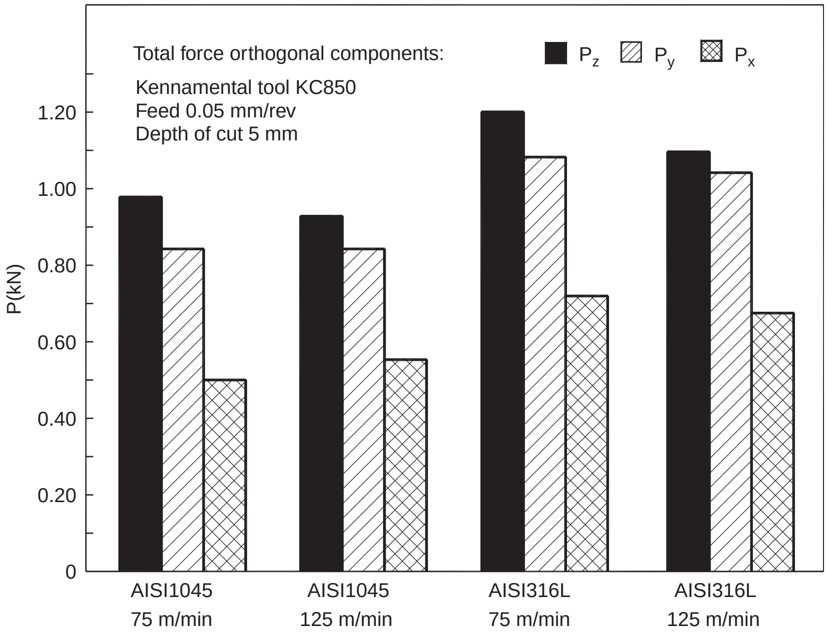

Fig. 8. Comparison of the cutting force components.

which determine the energy spent in deformation of the work material [25,49,75]. Only when the stress and corresponding strain are known, the other parameters-outcomes of the metal cutting process can be calculated [49].

4. Comparison of the known solutions for the single-shear plane model with experimental results

The next logical question is: How good is the single shear plane model? In other words, how far is this model from reality? Naturally, during the period of 1950–1960, when decent dynamometers and metallographic equipment became widely available, a number of fundamental works were carried out to answer this question. The results of these extensive researches are well summarized by Pugh [76] and Chisholm [77]. In the author's opinion, the best research results and a detailed description of the experimental methodology were presented by Pugh [76]. The results obtained by Pugh [76] was discussed by Bailey and Boothroyd ten years later [78]. In his study, all the possible 'excuses' for 'inadequate' experimental technique were eliminated. The experimental results are conclusively proved that for every work material tested, there is a marked disagreement in the 'φ vs. $(\mu-\gamma)$' relation between experiment and the predictions of the Ernest and Merchant, Merchant and the Lee and Shafer theories (Eqs. (5), (7) and (8), respectively). The examples of the obtained experimental results are shown in Figs. 9–12.

Fig. 9 shows experimental results for lead as the work material. Although such a choice of the work material might seem strange, one should realize that lead definitely has a significant advantage in cutting tests. This is because lead is chemically passive so it does not form solid state solutions and chemical compositions with common cutting tool materials. Therefore, the use of

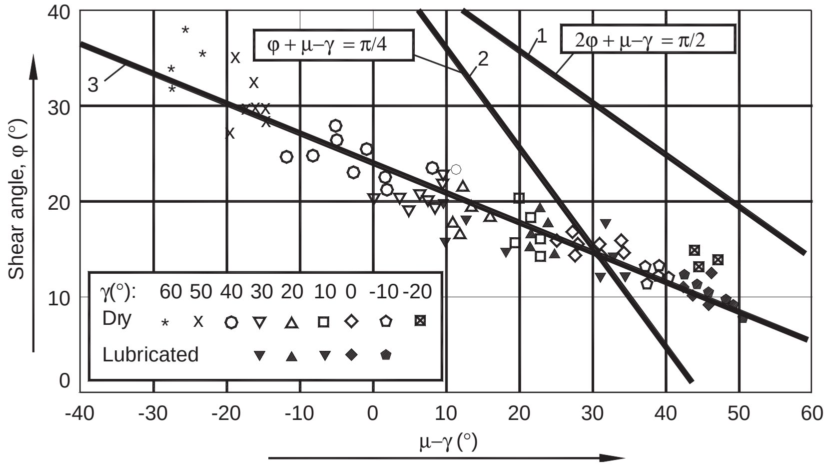

Fig. 9. Relation between φ and $(\mu - \gamma)$ for lead: 1—Ernst and Merchant solution, 2—Lee and Shafer solution, 3—experimental results.

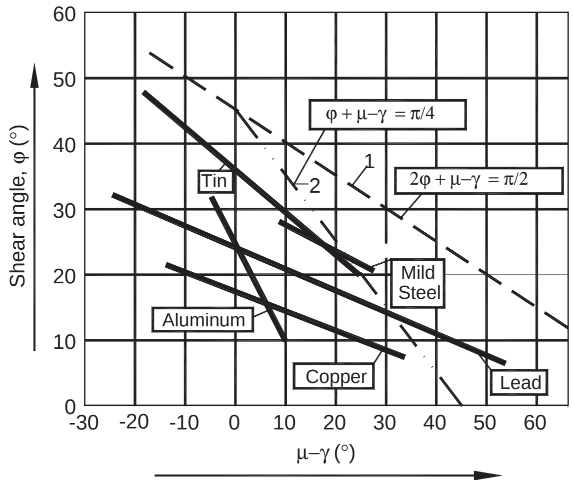

Fig. 10. Comparison between calculated and experimental results for tin, aluminum, mild steel, lead and copper.

lead as the work material allows to carry out much more "pure" cutting tests. In Fig. 9, line 1 graphically represents the Ernst and Merchant solution, 2—Lee and Shafer solution and 3—approximates the experimental results. Fig. 10 shows the results for the various tested work materials. As seen, the experimental results are not even close to those predicted theoretically. The similar conclusive results were presented by Creveling et al. [79] (an example is shown in Fig. 11 for steel 1113 where various cutting fluids were used) and by Chisholm [77].

The modified Merchant solution in which the shear stress is assumed to be linearly dependent on the normal stress through a factor $k_1(c = \cot^{-1} k_1)$ as

$$\tau = \tau_o + k_1 \sigma \tag{22}$$

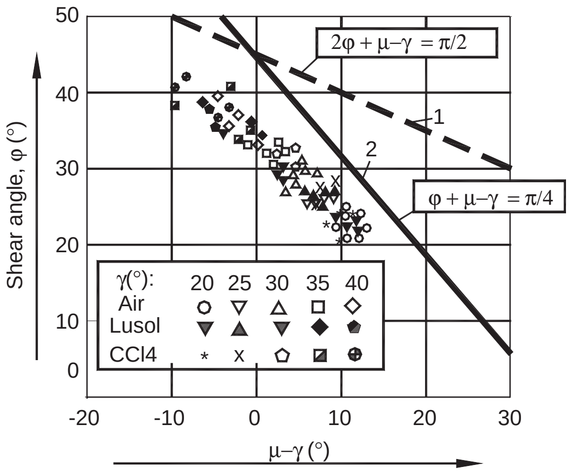

Fig. 11. Relation between φ and $(\mu - \gamma)$ for steel SAE 1113.

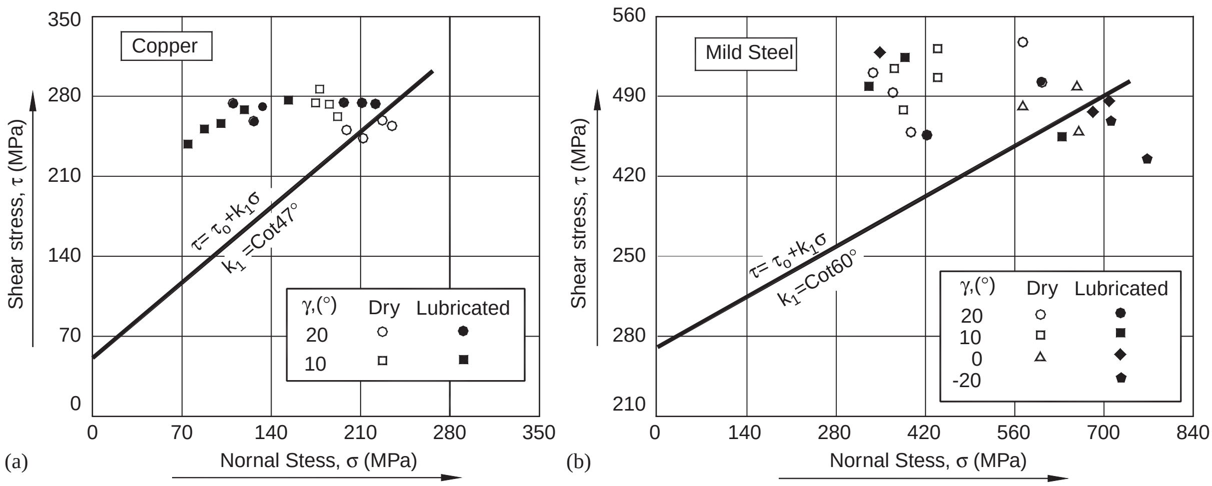

Fig. 12. Comparison between the estimated and experimentally obtained relationship "shear stress–normal stress" for copper (a) and steel (b).

(according to Merchant, τ_o and k_1 are work material constants) has also been examined for a wide variety of work materials. Eq. (22) is shown plotted in Fig. 12a and b for copper and mild steel, respectively, together with the experimentally obtained values [76]. As seen, the shear stress does not increase with the normal stress at the rate required by the modified Merchant solution, i.e. to fit experimental results. In fact, it would appear that the shear stress is almost independent of the normal stress on the single shear plane.

The above conclusions were confirmed by Bisacre [76] who conducted very similar cutting experiments. The results of these experiments enabled Bisacre to conclude that if the Merchant solution (theory) was correct, there would be a marked effect of the normal stress on the shear stress acting along the shear plane. To support his point, Bisacre noted that the results of tests carried out in which the same material was subjected simultaneously to torsion and axial compressions, showing that the shear strength of the material was almost independent of normal stress. As a result, the difference of the theoretical and experimental results cannot be attributed to the effect of the normal stress on the shear strength of the work material as suggested by Merchant.

Zorev also presented clear experimental evidences that the discussed solutions are inadequate [52]. He showed that Merchant solution is not valid even in the simplest case of cutting at low cutting speeds. Reading this, one may wonder why Zorev did not mention his findings about the single-shear plane model in his book [29] published 5 years later. In the author's opinion, if he had done so, he would have recognized that there was no available model of metal cutting at all. As a result, he included the above-discussed 'general solution' for the single-shear plane model 'forgetting' to mention that none of the possible particular solutions to this model is in any reasonable agreement with experimental results.

5. Conclusions

It is finally proven that there is a marked disagreement between the solutions available for the single-shear plane model and the experimental results. Hill, one of the founders of engineering plasticity [80], noticed [68] that "it is notorious that the extended theories of mechanics of machining do not agree well with experiment." Other prominent researchers in the field conclusively have proved that the experimental results are not even close to those predicted theoretically [52,76,77,79]. Recent researches further clarified this issue presenting more theoretical and experimental evidences [38,75,81].

As one might expect, knowing these results, the single-shear plane model would be just a part of the history. In reality, however, this is not the case and the single-shear plane model managed to 'survive' all these conclusive facts and is still the first choice for practically all the textbooks on metal cutting used today [10–12,42,72,82–84]. In contrary, all the excellent works showing complete disagreement of this model with reality are practically forgotten and not even mentioned in modern metal cutting books, which still discuss the single-shear plane model as the very core of the metal cutting theory. Moreover, the book "Application of Metal Cutting Theory" [11] is entirely based on this model showing how to apply it in practical calculations although other research works complain about the absence of "the predictive theory or analytical system which enables us, without any cutting experiment, to predict cutting performance such as chip formation, cutting force, cutting temperature, tool wear, and surface finish" [2]. It should become clear that any progress in the prediction ability of the metal cutting theory cannot be achieved if the single-shear plane model is still used.

It is instructive to list the major drawbacks of the single-shear plane model:

Inherent drawbacks

- *Infinite strain rate*. Infinite deceleration and thus strain rate of a microvolume of the work material passing through the shear plane.

- *Unrealistically high shear strain*. The calculated shear strain in metal cutting is much greater than the strain at fracture achieved in the mechanical testing of materials under various conditions. Moreover, when the chip compression ratio $\zeta = 1$, i.e. the uncut chip thickness is equal to the chip thickness, no plastic deformation occurs in metal cutting. [49], the shear strain, calculated by the model remains very significant without any apparent reason for that.
- *Unrealistic behavior of the work material*. Rigid perfectly plastic work material is assumed which is not the case in practice.
- *Improper accounting for the resistance of the work material to cut*. The shear strength or the flow shear stress cannot be considered as an adequate characteristic in this respect because, considered alone, the stress does not account for the energy spent in cutting.
- *Unrealistic representation of the tool-workpiece contact*. The cutting edge is perfectly sharp and no contact takes place on the tool flank surface. This is in obvious contradiction with the practice of machining where the flank wear (due to the tool flank-workpiece contact) is a common criterion of tool life [85].
- *Inapplicability for cutting brittle work materials*. Model is not applicable for the case of the cutting of brittle materials, which exhibit no or very little plastic deformation by shear. Nevertheless, the single-shear model is still applied to model the machining of gray cast iron [86], cryogenic water ice [87], etc.

Ernst and Merchant induced drawbacks

- *Incorrect velocity diagram*. In the known considerations of velocities in metal cutting, the common coordinate system is not set, so that the existing velocity diagram consists of the velocity components from different coordinate systems. As a result, unrealistic velocity components are considered.
- *Incorrect force diagram*. The bending moment due to the parallel shift of the resultant cutting force is missed in the force diagram. As shown [25], this missed moment is the prime cause for chip formation and thus it distinguishes the cutting process among other deforming processes. Moreover, the state of stress imposed by this moment in the chip root causes chip curling.
- *Constant friction coefficient*. Because the friction coefficient at the tool–chip interface can be thought as the ratio of the shear and normal force on this interface, the distributions of the normal and shear stresses should be equidistant over this interface. The available theoretical and experimental data [12,29,43,54–56,83,88] do not conform this assumption.

References

[1] Usui E, Shirakashi T. Mechanics of metal cutting—from ''description'' to ''predictive'' theory. In: On the art of cutting metals—75 years later. Phoenix, USA: Production Engineering Division (PED), ASME; 1982.

[2] Usui E. Progress of ''predictive'' theories in metal cutting. JSME International Journal 1988;31:363–9.

[3] Armarego EJA. Predictive modeling of machining operations—a means of bridging the gap between the theory and practice—a keynote paper. In: The 13th symposium on engineering applications of mechanics. Hamilton, ON, Canada: CMSE; 1996.

[4] Endres WJ, Devor RE, Kapoor SG. A dual-mechanism approach to the prediction of machining forces, part 1: model development. ASME Journal of Engineering for Industry 1995;117:526–33.

[5] Kopac J, Dolinsek S. Advantages of experimental research over theoretical models in the field of metal cutting. Experimental Techniques 1996;20:24–8.
[6] Armarego EJ, Brown RH. The machining of metals. New Jersey, USA: Prentice-Hall; 1969.
[7] Shaw MC. Metal cutting principles, 2nd ed. Oxford: Oxford University Press; 2005.
[8] AdvantEdge(tm) Modelingsoftware. Thirdwavesystems, (http://www.thirdwavesys.com), 2004.
[9] DeGarmo EP, Black JT, Kohser RA. Materials and processes in manufacturing, 9th ed. New York: Wiley; 2003.
[10] Kalpakjian S, Schmid SR. Manufacturing engineering and technology. New Jersey: Prentice-Hall; 2001.
[11] Gorczyca FY. Application of metal cutting theory. New York: Industrial Press; 1987.
[12] Shaw MC. Metal cutting principles. Oxford: Oxford Science Publications; 1984.
[13] Jawahir IS, Balaji AK, Stevenson R, van Luttervelt CA. Towards predictive modeling and optimization of machining operations. In: Manufacturing science and engineering. Proceedings of the 1997 ASME international mechanical engineering congress and exposition. Dallas, TX: ASME; 1997.
[14] Jawahir IS, Zhang JP. An analysis of chip curl development, chip deformation and chip breaking in orthogonal machining. Transactions of NAMRI/SME, vol. XXIII; 1995. p. 109–14.
[15] Fang N, Jawahir IS, Oxley PLB. A universal slip-line field model with non-unique solutions for machining with curled chip formation and a restricted contact tool. International Journal of Mechanical Sciences 2001;43:557–80.
[16] Fang N, Jawahir IS. Analytical predictions and experimental validation of cutting force ratio, chip thickness, and chip back-flow angle in restricted contact machining using the universal slip-line model. International Journal of Machine Tools and Manufacturing 2002;42:681–94.
[17] Fang N, Jawahir IS, Oxley PLB. A universal slip-line model with non-unique solutions for machining with curled chip formation and a restricted contact tool. International Journal of Mechanical Sciences 2001;43:557–80.
[18] Finnie I. Review of the metal-cutting analysis of the past hundred years. Mechanical Engineering 1956;78:715–21.
[19] Piispanen V. Lastunmuodostumisen teoriaa. Teknillinen Aikakauslehti 1937;27:315–22.
[20] Piispanen V. Theory of formation of metal chips. Journal of Applied Physics 1948;19:876–81.
[21] Oxley PLB. Mechanics of machining: an analytical approach to assessing machinability. New York, USA: Wiley; 1989.
[22] Time I. Resistance of metals and wood to cutting. St. Petersbourg, Russia: Dermacow Press House; 1870 [in Russian].
[23] Tresca H. Mémores sur le Rabotage des Metaux. Bulletin de la Société d'Encouragement pour l'Industrie Nationale 1873;15:585–685.
[24] Time I. Memore sur le Rabotage de Métaux. Russia: St. Petersbourg; 1877.
[25] Astakhov VP. Metal cutting mechanics. Boca Raton, USA: CRC Press; 1998.
[26] Zvorykin KA. On the force and energy needed to separate the chip from the workpiece. 1896;123:57–96 [in Russian].
[27] Boston OW. A bibliography on cutting of metals. New York: ASME; 1945.
[28] Briks AA. Metal cutting. Publ. House; 1896 [in Russian].
[29] Zorev NN, editor. Metal cutting mechanics. Oxford: Pergamon Press; 1966.
[30] Johnson W, Mellor PB. Engineering plasticity. London, Inglaterra: Van Nostrand Reinhold Company; 1973.
[31] Palmer WB, Oxley PLB. Mechanics of metal cutting. Proceedings of the Institution of Mechanical Engineers 1959;173:557–80.
[32] Kudo H. Some new slip-line solutions for two-dimensional steady-state machining. International Journal of Mechanical Sciences 1965;7:43–55.
[33] Okushima K, Hitomi K. An analysis of the mechanism of orthogonal cutting and its application to discontinuous chip formation. ASME Journal of Engineering for Industry 1961;83:545–56.
[34] Ernst H, Merchant ME. Chip formation, friction and high quality machined surfaces. Surface treatment of metals. ASM 1941;29:299–378.
[35] Merchant ME. Mechanics of the metal cutting process. I. Orthogonal cutting and a type 2 chip. Journal of Applied Physics 1945;16:267–75.
[36] Lee EH, Shaffer BW. The theory of plasticity applied to a problem of machining. Journal of Applied Mechanics 1951;18:405–13.
[37] Reuleaux F. Über den taylor whiteschen werkzeugstahl verein sur berforderung des gewerbefleissen in preussen. Sitzungsberichete 1900;79:179–220.

[38] Atkins AG. Modelling metal cutting using modern ductile fracture mechanics: qualitative explanations for some longstanding problems. International Journal of Mechanical Sciences 2003;45:373–96.
[39] DeGamo EP, Black JT, Kohser RA. Materials and processing in manufacturing. New York: Macmillan; 1988.
[40] Astakhov VP, Osman MOM, Hayajneh MT. Re-evaluation of the basic mechanics of orthogonal cutting: velocity diagram, virtual work equation and upper-bound theorem. International Journal of Machine Tools & Manufacturing 2001;41:393–418.
[41] Black JT, Huang JM. Shear strain model in metal cutting. Manufacturing Science and Engineering 1995;MED-Vol.2-1:283–302.
[42] DeGarmo EP, Black JT, Kohser RA. Materials and processes in manufacturing. Upper Saddle River, NJ: Prentice-Hall; 1997.
[43] Altintas Y. Manufacturing automation. Metal cutting mechanics, machine tool vibrations, and CNC design. Cambridge: Cambridge University Press; 2000.
[44] Stenphenson DA, Agapiou JS. Metal cutting theory and practice. New York: Marcel Dekker; 1996.
[45] Vyas A, Shaw MC. Mechanism of saw-tooth chip formation in metal cutting. ASME Journal of Manufacturing Science and Engineering 1999;121:163–72.
[46] Field JE, Walley SM, Proud WG, Goldrein HT, Siviour CR. Review of experimental techniques for high rate deformation and shock studies. International Journal of Impact Engineering 2004;30:725–75.
[47] Rohr I, Nahme H, Thoma K. Material characterization and constitutive modelling of ductile high strength steel for a wide range of strain rates. International Journal of Impact Engineering 2005;31(4):401–33.
[48] Tönshoff HK, Amor RB, Andrae P. Chip formation in high speed cutting (HSC), SME paper MR99-253. Dearborn MI: SME; 1999.
[49] Astakhov VP, Shvets S. The assessment of plastic deformation in metal cutting. Journal of Materials Processing Technology 2004;146:193–202.
[50] Payton LN, Black JT. Low speed orthogonal machining of copper with hardness gradient. SME Technical Paper MR01-266; 2001. p. 1–8.
[51] Dieter G. Mechanical metallurgy. New York: McGraw-Hill; 1976.
[52] Zorev NN. Results of work in the field of the mechanics of the metal cutting process. Proceedings of the IME conference on technical engineering manufacture, London; 1958.
[53] Astakhov VP, Outeiro JC. Modeling of the contact stress distribution at the tool–chip interface. Machining Science and Technology 2005;9:85–99.
[54] Poletica MF. Contact loads on tool interfaces. Moscow: Mashinostroenie; 1969 [in Russian].
[55] Loladze TN. Strength and wear of cutting tools. Moscow: Mashgiz; 1958 [in Russian].
[56] Kronenberg M. Machining science and application. Theory and practice for operation and development of machining processes. Oxford: Pergamon Press; 1966.
[57] Finnie I, Shaw MC. The friction process in metal cutting. Transactions of ASME 1956;77:1649–57.
[58] Usui E, Takeyma H. A photoelastic analysis of machining stresses. ASME Journal of Engineering for Industry 1960;81:303–8.
[59] Strenkowski JS, Moon K-J. Finite element prediction of chip geometry and tool/workpiece temperature distributions in orthogonal metal cutting. ASME Journal of Engineering for Industry 1990;112:313–8.
[60] Komvopoulos K, Erpenbeck SA. Finite element modeling of orthogonal metal cutting. ASME Journal of Engineering for Industry 1991;113:253–67.
[61] Lin ZC, Pan WC, Lo SP. A study of orthogonal cutting with tool flank wear and sticking behaviour on the chip–tool interface. Journal of Materials Processing Technology 1995;52:524–38.
[62] Lin ZC, Lin SY. A coupled finite element model of thermo-elastic-plastic large deformation for orthogonal cutting. Journal of Engineering Materials and Technology 1992;114:218–26.
[63] Strenkowski JS, Carroll JT. A finite element model of orthogonal metal cutting. ASME Journal of Engineering for Industry 1985;107:349–54.
[64] Endres WJ, Devor RE, Kapoor SG. A dual-mechanism approach to the prediction of machining forces. Part 2: calibration and validation. ASME Journal of Engineering for Industry 1995;117:534–41.
[65] Olovsson L, Nilsson L, Simonsson K. An ALE formulation for the solution of two-dimensional metal cutting problems. Computers and Structures 1998;72:497–507.

[66] Kronenberg M. Machining science and application. Theory and practice for operation and development of machining processes. Oxford: Pergamon Press; 1966.
[67] Astakhov VP. Tribology of metal cutting. In: Totten HL, GE, editor. Mechanical tribology. New York: Marcel Dekker; 2004. p. 307–46.
[68] Hill R. The mechanics of machining: a new approach. Journal of the Mechanics and Physics of Solids 1954;3:47–53.
[69] Rubenstein C. A note concerning the inadmissibility of applying of minimum work principle to metal cutting. ASME Journal of Engineering for Industry 1983;105:294–6.
[70] Dewhurst W. On the non-uniqueness of the machining process. Proceedings of the Royal Society of London A 1978;360:587–609.
[71] Ernst H. Physics of metal cutting. Cincinnati, OH, USA: The Cincinnati Milling Machine Co.; 1938.
[72] Trent EM, Wright PK. Metal cutting. Boston: Butterworth-Heinemann; 2000.
[73] Astakhov VP. A treatise on material characterization in the metal cutting process. Part 2: cutting as the fracture of workpiece material. Journal of Materials Processing Technology 1999;96:34–41.
[74] Outeiro JC. Application of recent metal cutting approaches to the study of the machining residual stresses. Coimbra: Department of Mechanical Engineering, University of Coimbra; 2003. p. 340.
[75] Astakhov VP. Chapter 9: Tribology of metal cutting. In: Liang GTAH, editor. Mechanical tribology, material characterization and application. New York: Marcel Dekker; 2004. p. 307–46.
[76] Pugh HLD. Mechanics of metal cutting process. In: Proceedings of the IME conference on technical engineering manufacture, London; 1958.
[77] Chisholm AWJ. A review of some basic research on the machining of metals. In: Proceedings of the IME conference on technical engineering manufacture, London; 1958.
[78] Bailey JA, Boothroyd G. Critical review of some previous work on the mechanics of the metal-cutting process. ASME Journal of Engineering for Industry 1969;90:54–62.
[79] Creveling JH, Jordon TF, Thomsen EG. Some studies on angle relationship in metal cutting. ASME Journal of Applied Mechanics 1958;79:127–38.
[80] Hill R. The mathematical theory of plasticity. London: Oxford University Press; 1950.
[81] Atkins AG, Mai YW. Elastic and plastic fracture: metals, polymers. Ceramics, composites, biological materials. New York: Wiley; 1985.
[82] Boothroyd G, Knight WA. Fundamentals of machining and machine tools, 2nd ed. New York: Marcel Dekker; 1989.
[83] Childs THC, Maekawa K, Obikawa T, Yamane Y. Metal machining. Theory and application. London: Arnold; 2000.
[84] Ivester RW, Kennedy M, Davies M, Stevenson RJ, Thiele J, Furness R, Athavale S. Assessment of machining models: progress report. In: Proceedings of the third CIRP international workshop on modelling of machining operations. Sydney, Australia: University of New South Wales; 2000.
[85] Astakhov VP. The assessment of cutting tool wear. International Journal of Machine Tools and Manufacture 2004;44:637–47.
[86] Eleftherion E, Bates CE. Effect of inoculation on machinability of gray cast iron. ASF Transactions 1999;122:659–69.
[87] Garry JRC, Wright IP. The cutting strength of cryogenic water. England: Ice Planetary Science Research Institute, Open University; 2000.
[88] Astakhov VP, Outeiro JC. Modeling of the contact stress distribution at the tool–chip interface. In: Proceeding of the seventh CIRP international workshop on modeling of machining operations. Cluny, France: ENSAM; 2004.